Draft version September 24, 2009
Preprint typeset using LaTeX style emulateapj v. 08/22/09

BROADBAND IMAGING SEGREGATION OF $z \sim 3$ Lyα EMITTING AND Lyα ABSORBING GALAXIES

Jeff Cooke[1,2]
The Center for Cosmology and the Department of Physics & Astronomy, The University of California, Irvine, Irvine, CA, 92697-4575
Draft version September 24, 2009

ABSTRACT

The spectral properties of Lyman break galaxies (LBGs) offer a means to isolate pure samples displaying either dominant Lyα in absorption or Lyα in emission using broadband information alone. We present criteria developed using a large $z \sim 3$ LBG spectroscopic sample from the literature that enables large numbers of each spectral type to be gathered in photometric data, providing good statistics for multiple applications. In addition, we find that the truncated faint, blue-end tail of $z \sim 3$ LBG population overlaps and leads directly into an expected Lyα emitter (LAE) population. As a result, we present simple criteria to cleanly select large numbers of $z \sim 3$ LAEs in deep broadband surveys. We present the spectroscopic results of 32 $r' \lesssim 25.5$ LBGs and $r' \lesssim 27.0$ LAEs at $z \sim 3$ pre-selected in the Canada-France-Hawaii Telescope Legacy Survey that confirm these criteria.

Subject headings: galaxies: evolution — galaxies: formation — galaxies: fundamental parameters — galaxies: photometry

1. INTRODUCTION

The Lyman break galaxies (LBGs; Steidel et al. 1996) are a high-redshift population of star forming galaxies selected by their rest-frame ultraviolet colors. LBGs at $z \sim 3$ are faint ($L*$ corresponds to $m_R \sim 24.5$ at $z \sim 3$) and require long integrations using 8 m class telescopes to obtain spectral information having a signal-to-noise ratio (S/N) of a few. Nevertheless, > 1500 $z \sim 3$ spectra have been obtained and studied (e.g., Le Fèvre et al. 2005; Cooke et al. 2005; Steidel et al. 2003, hereafter CCS03). Lyα is the most prominent feature in LBG spectra and has been shown to be indicative of other spectral properties, such as interstellar medium absorption line strength and continuum profile (Shapley et al. 2003, hereafter AES03).

Inspection of the spectroscopic samples gathered to date show that $\sim 50\%$ of LBGs exhibit dominant (or net) Lyα in absorption, with the remaining exhibiting dominant Lyα in emission (e.g., AES03 Cooke et al. 2005). A recent investigation of close and interacting pairs (Cooke et al. 2009a) finds evidence of an overabundance of $z \sim 3$ LBGs exhibiting Lyα emission in close pairs; all LBGs with projected physical separations $\lesssim 15$ h^{-1}kpc display Lyα in emission. To properly explore this relationship, along with other spectroscopic trends with spatial distribution, large samples that reflect the spectral properties of LBGs are necessary. However, the conventional means of multi-object spectroscopy is inefficient in acquiring the spectra of galaxies closely spaced on the sky because of inherent mechanical constraints (see Cooke et al. 2009a). As a result, comprehensive LBG spectroscopic surveys are difficult and time intensive.

High-redshift star-forming systems with continua typically too faint for spectroscopic follow-up, but with prominent Lyα emission (Cowie & Hu 1998; Hu et al. 1998), have been detected via targeted spectroscopic and narrowband surveys (e.g., Dawson et al. 2004; Ouchi et al. 2005; Venemans et al. 2005; Gawiser et al. 2006). Because of the faint continua of these Lyα emitters (LAEs), and the difficulties involved in their acquisition, LAE surveys have been limited to narrow redshift ranges and typically clustered fields. As a result, fewer total spectra have been compiled relative to LBGs, with the details of the process, or processes, that contribute to the generation and escape of Lyα emission, less certain. In addition, the data-gathering techniques have provided only a few cases to date where the mass of LAEs from clustering can be reasonably inferred (Ouchi et al. 2003; Shimasaku et al. 2004; Kovač et al. 2007; Gawiser et al. 2007).

LBGs at $z \sim 3$ that are dominated by Lyα in absorption separate sufficiently in color–magnitude space from those dominated by Lyα in emission to enable a simple means using broadband imaging to isolate subsets with desired Lyα features and associated spectral properties. Furthermore, we find that deep broadband criteria can select clean, EW unbiased samples of $z \sim 3$ LAEs with photometrically detectable continua. As a result, very large numbers $z \sim 3$ systems over defined volumes with desired spectral properties can be efficiently obtained for statistical study, complementing the limitations of narrowband surveys and extensive deep spectroscopic campaigns. We describe the observations used in this work in Section 2. In Section 3, we present the behavior of LBG spectroscopic subsets, the criteria for LBG spectral-type and LAE selection, and the results of our spectroscopic test of the criteria. Finally, we provide a conclusion in Section 4. Magnitudes presented here are in the AB (Fukugita et al. 1996) magnitude system.

2. OBSERVATIONS

We use the publicly available data set of CCS03 [3] and related accessible files to quantify the spectroscopic prop-

Electronic address: cooke@uci.edu
[1] California Institute of Technology, MC 249-17, 1200 E. California Blvd., Pasadena, CA 91125
[2] Gary McCue Postdoctoral Fellow

[3] http://vizier.cfa.harvard.edu/viz-bin/VizieR?-source=J/ApJ/592/728/

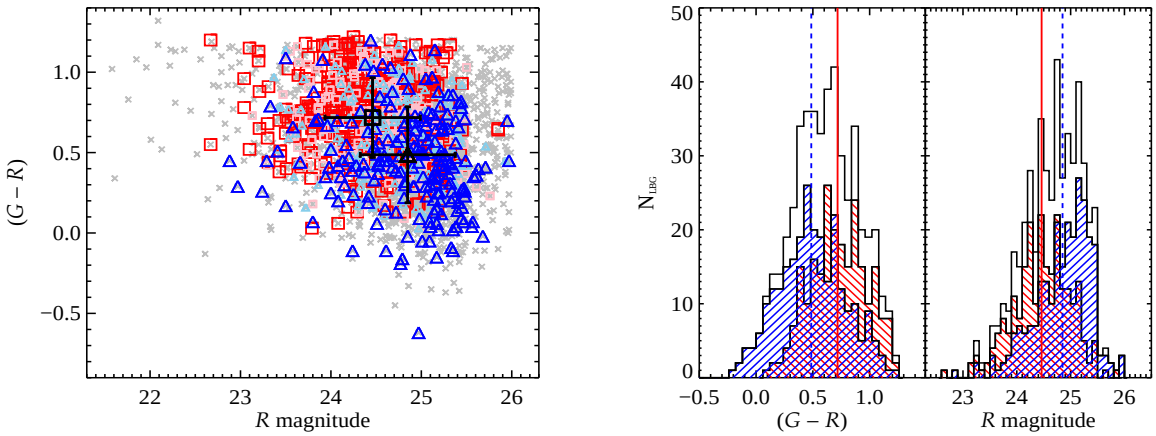

FIG. 1.— Left panel: color-magnitude diagram of $z \sim 3$ LBGs in the Steidel et al. (2003) sample. Photometrically selected galaxies are plotted as gray crosses, whereas spectroscopically confirmed $z \sim 3$ LBGs are the larger (colored) symbols coded by their Lyα EW and represent the four quartiles as defined in Shapley et al. (2003). Specifically, group 1 – large *(gray/red)* squares, group 2 – small *(gray/pink)* squares, group 3 – small *(black/light blue)* triangles, and group 4 – large *(black/blue)* triangles. The large square and triangle and associated error bars represent the mean and 1σ standard deviation for the distributions of LBGs with net Lyα in absorption (aLBGs) and net Lyα in emission (eLBGs), respectively. Right two panels: histograms of the aLBG (*(gray/red)*, back-hatched) and eLBG (*(black/blue)*, forward-hatched) $(G - \mathcal{R})$ color and $\mathcal{R}$ mag distributions (see the text). The $(G - \mathcal{R})$ color-selection criteria omit the far red tail of the aLBG distribution in an effort to avoid low-redshift interlopers. The spectroscopic-justified magnitude truncation ($\mathcal{R} \leq 25.5$) of eLBGs suggests that a continuation of this distribution probes a Lyα emitter population.

erties of $z \sim 3$ LBGs and establish the $U_nG\mathcal{R}$ spectral-type selection criteria. This survey consists of ~ 2500 $U_nG\mathcal{R}$ selected and ~ 800 spectroscopically confirmed LBGs from 17 separate fields that effectively sample the $z \sim 3$ LBG population as a whole. As a key component to this work, we use the Lyα EW measurements of AES03 for 775 LBG spectra of the CCS03 sample (A. E. Shapley, 2009, private communication).

In Section 3.3, we test the criteria presented below using the spectra of 32 u^*gi-selected $z \sim 3$ LBGs in the Canada France Hawaii Telescope Legacy Survey (CFHTLS) Deep field "D4" [4]. We r-band select $z \sim 3$ LBGs from stacked images that combine four years of high-quality observations that reach limiting magnitudes of $u^* \sim 27.5, g \sim 27.5, r \sim 27.0$, and $i \sim 26.7$. The stacked r-band images probe $\gtrsim 1.0-1.5$ mag deeper than the $\mathcal{R}$-band images of CCS03 and thereby test a fainter regime. The $z \sim 3$ LBG criterion $(u^*-g) \geq 1.25(g-i)$ for the CFHT Megacam filters imposes a weaker restriction on the u^*-band depth as compared to the $(U_n-G) \geq (G-\mathcal{R})+1.0$ criteria of CCS03. This minimizes the introduction of a bias in $r > 25.5$ LBG selection based on their $(g-i)$ colors. For further information on image stacking and color-selection spectroscopic tests, see Cooke et al. (2009b, Supplementary Information).

We acquired the spectroscopic data using the Low-Resolution Imaging Spectrometer (LRIS; Oke et al. 1995; McCarthy et al. 1998) mounted on the Keck I telescope on 2009 July 20 using the 400/3400 grism on the new blue arm and 400/8500 grating on the new red arm yielding a blue/red resolution of ~ 300 km s^{-1}. Time constraints resulted in a total integration time of 3600s with $\sim 0.''9$ seeing FWHM. This is a $\sim 0.5\times$ the total

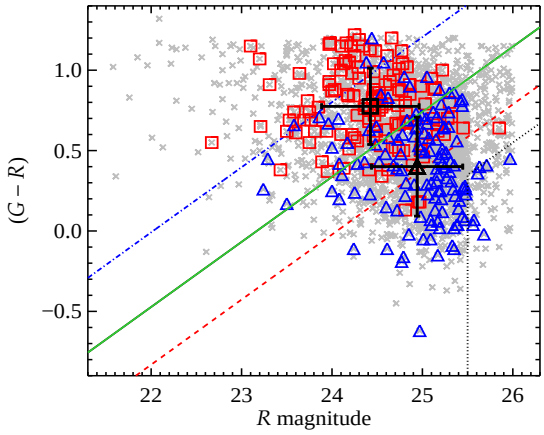

FIG. 2.— Similar to Figure 1, but for LBGs that exhibit the opposite extremes in Lyα features and associated spectral profiles. Squares denote the subset of 150 LBGs that display the strongest Lyα absorption and triangles denote the subset of 150 LBGs that display the strongest Lyα emission. The solid (green) line denotes our primary statistical cut of the two distributions and is the basis for subsequent selection criteria. The dashed (red) and dot-dashed (blue) lines indicate a $(G-\mathcal{R})$ distribution 1.5σ separation from the primary cut for the Lyα absorber and Lyα emitter subsets, respectively. This corresponds to $\gtrsim 2.5\sigma$ from each of the respective $(G-\mathcal{R})$ and $\mathcal{R}$ distribution mean values. Objects beyond these cuts produce $\gtrsim 90\%$ pure samples of either spectral type. Objects fainter than $\mathcal{R} = 25.5$ that lay $\geq 3\sigma$ from the aLBG color distribution mean value comprise an expected population of LAEs. This region is shown bounded by dotted lines.

[4] http://www1.cadc-ccda.hia-iha.nrc-cnrc.gc.ca/cadcbin/cfht/wdbi.cgi/cfht/tpx_fields/form

integration time of typical $z \sim 3$ LBG spectroscopy, but is found to be sufficient to identify most $\mathcal{R} \gtrsim 25.5$ candidates and the Lyα emission feature of $\mathcal{R} \gtrsim 27.0$ LAEs.

3. ANALYSIS

We construct a $(G - \mathcal{R})$ versus $\mathcal{R}$ color–magnitude diagram (CMD) for the CCS03 LBG photometric sample, plotted in the left panel of Figure 1. Motivated by the results of Cooke et al. (2009a), we overlay the spectroscopically confirmed LBGs and code them by their AES03 defined Lyα EW quartiles. AES03 find that LBGs with strong Lyα have blue $\sim 1300 - 2000$Å continua with a continuous reddening trend seen with decreasing Lyα emission EW, through to strong absorption. This is the main cause of the color separation on the CMD in Figure 1. The presence of the Lyα feature in the G band also contributes to the color separation, but to a lesser extent, and is on order of the $\lesssim 0.2$ mag uncertainties.

We use the term "aLBGs " for LBGs with dominant Lyα in absorption (net Lyα EW < 0) and "eLBGs" for dominant Lyα in emission (net Lyα EW > 0). We find that the aLBG and eLBG distributions show significant overlap but are distinct populations. A two-sided K–S test of the aLBG and eLBG $(G - \mathcal{R})$ distributions produces a probability of $p = 1.5 \times 10^{-13}$ that the two distributions are pulled from the same population. Similarly, a K–S test produces $p = 3.0 \times 10^{-13}$ for the $\mathcal{R}$ mag distributions. This is illustrated in the right panels of Figure 1.

Next, we study two LBG spectral subsets that exhibit the opposite extremes in Lyα EW behavior. Subset 1 contains the 150 strongest aLBGs (net Lyα EW ≤ -12.0) and subset 2 consists of the 150 strongest eLBGs (net EW ≥ 26.5) of the full spectroscopic sample. The $(G - \mathcal{R})$ versus $\mathcal{R}$ CMD of the two subsets is plotted in Figure 2 and shows two cohesive distributions with a more distinct separation when compared to the aLBG/eLBG distribution values shown in Figure 1. Using the statistical mean values of the two subsets, we sever the populations in both color and magnitude as shown by the solid line in Figure 2. This line falls $\sim 1\sigma$ from both the color and magnitude mean values of both distributions and defines our primary cut. We show that more restrictive selections based on the slope of this cut (defined below), are very effective in isolating LBG spectral types with differing Lyα and continuum profiles.

3.1. *Spectral-Type Selection Criteria*

We use the parameters of the subset 1 and 2 distributions to refine the primary cut in an effort to generate pure samples of each spectral type. Choosing CMD cuts that are separated from the primary cut by 1.5σ of the $(G - \mathcal{R})$ distributions of each subset and along the same slope as the primary cut, selects LBG spectral types $\gtrsim 2.5\sigma$ from the mean values of the opposite distribution. We find that the following criteria select nearly pure samples of aLBGs:

$$(G - R) \;\geq\; 0.4047\; R - 9.376 + 1.5\sigma_A, \qquad (1)$$

and eLBGs

$$(G - R) \;\leq\; 0.4047\; R - 9.376 - 1.5\sigma_E, \qquad (2)$$

where $\sigma_A = 0.3095$ and $\sigma_E = 0.2392$ and are the 1σ standard deviations of the $(G - \mathcal{R})$ distributions for subset 1 and subset 2, respectively. These selection cuts are indicated in Figure 2.

Applying Equations 1 and 2 to the full spectroscopic data set of CCS03 produces spectral-type samples consisting of 40 aLBGs and 60 eLBGs with contamination fractions of 0.100 and 0.067, respectively (Figure 3; top panel). In addition, Figure 3 presents the net Lyα EW and redshift distributions for the two isolated samples (center and bottom panels, respectively). The samples exhibit 66 ± 36 Å EW for the eLBGs and -20 ± 10 Å EW for the aLBGs and their redshift distributions are found to be representative of the full data set ($z_{FULL} = 2.97 \pm 0.27$, $z_{aLBG} = 3.05 \pm 0.25$, and $z_{eLBG} = 2.88 \pm 0.24$). The above criteria, of course, can be made more strict by using a larger coefficient of σ_A and σ_E, thereby producing samples that are more pure, at the cost of sample size. In this manner, large photometric data sets can obtain very clean spectral-type samples while still maintaining a large number of objects for good statistics.

3.2. *Lyα emitters*

LAEs at $z \sim 3$ have colors similar to eLBGs with the bulk expected to have $(G - \mathcal{R}) \lesssim 0.0$ (see Reddy & Steidel 2009, Appendix A). The colors and mass of LAEs (e.g., Gawiser et al. 2007; Lai et al. 2008) appear to provide a natural extension of the LBG population and would help to complete the $\mathcal{R} \sim 25.5$ eLBG magnitude truncation.

From the aLBG/eLBG color and magnitude distributions and those of their spectral subsets, and the results of the spectral-type selection criteria above, we find that a pure sample of LAEs (defined here as having $\mathcal{R} > 25.5$) can be obtained using

$$(G - R) \;\leq\; 0.4047\; R - 9.376 - 2.0\sigma_E \text{ and } R \geq 25.5, \qquad (3)$$

which modifies the eLBG cut to a larger separation from the primary cut. This effectively avoids systems displaying Lyα in absorption by selecting objects $\gtrsim 3\sigma$ from the mean of the aLBG distribution. The region of the CMD defined by Equation 3 is indicated in Figure 2 and shows that the few spectroscopically identified objects in the CCS03 sample that meet these criteria exhibit Lyα in emission. Similar to above, the purity of the LAE sample can be determined by the σ_E coefficient.

3.3. *Spectroscopic Tests of the Spectral-Type Predictions*

We use 34316 u^*gi-selected $z \sim 3$ LBGs in the CFHTLS Deep field "D4" to test the predictions of the spectral-type criteria and our LAE assumptions. Figure 4 plots the $(g - i)$ versus i mag CMD for the "D4" field and shows our tentative spectral-type cuts based on the $r < 25.5$ $z \sim 3$ LBG densities and the results of the above analysis. The primary cut shown here produces aLBG/eLBG samples with a very similar $r \leq 25.5$ ratio ($\sim 4600/5200$) as compared to the $\mathcal{R}$ ratio of CCS03 when maintaining conventional color-selection criteria, and specifically the constraint $(g - i) \geq -0.2$. For more complete color-space detection, we relax the criterion to $(g - i) \geq -1.0$ to include the small number of bluer objects to probe the full eLBG and expected LAE $(g - i)$ distribution. The relaxation of the color in this manner does not increase the fraction of interlopers (e.g., CCS03; Cooke et al. 2005). The "D4" field is reflective

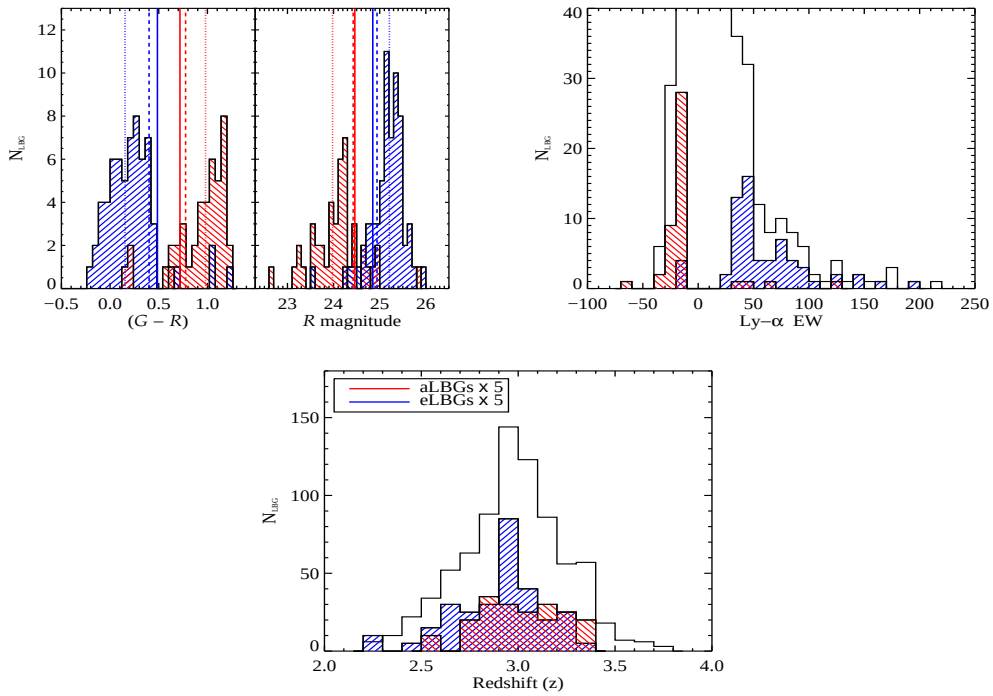

FIG. 3.— Histograms of the isolated spectral-type samples obtained when applying Equations 1 and 2 to the spectroscopic dataset of Steidel et al. (2003). Top: the back-hatched and forward-hatched histograms indicate the $\gtrsim 90\%$ pure aLBG and eLBG isolated spectral-type samples, respectively. In each sample gray (red) denotes aLBGs and black (blue) denotes eLBGs. Vertical lines mark the mean values of the aLBG/eLBG ((gray/red; black/blue) solid), subset 1/subset 2 ((gray/red; black/blue) dashed), and spectral-type sample [(gray/red; black/blue) dot-dash] distributions. Center: the net Lyα EW distribution for the total spectroscopic data set (unfilled; see Shapley et al. (2003) for the full-scale histogram) and the isolated spectral-type samples. Bottom: the redshift distribution of the full sample (unfilled) and the isolated spectral-type samples scaled by a factor of 5 to better compare the form of the distributions (i.e., any difference between the isolated samples and the isolated samples and the full sample is amplified by a factor of 5).

of the remaining three CFHTLS Deep fields in depth and generates spectral-type samples of $\sim$ 1600 aLBGs and $\sim 14,000$ eLBGs, $\sim$ 8000 of which fall in the LAE selection region (LAE magnitude definition shown in Figure 4 is $i > 25.5$).

The analysis of our 32 spectra (Section 2) indicates that our tentative spectral-type cuts are very effective. Of the 11 LBGs targeted in the aLBG spectral-type cut, eight have confirmed Lyα in absorption, two show complex absorption and emission profiles with net Lyα emission, and one is unidentified as a result of its low S/N. Nine of the 17 LBGs targeted in the eLBG region were unidentified (although six show weak evidence of emission), with eight exhibiting Lyα emission. Seven of the eight galaxies that fall in the LAE region show Lyα emission, with the remaining galaxy being unidentified. This demonstrates a high efficiency in identifying $i \lesssim 27.0$ LAEs from their broadband colors and helps to confirm the LAE extension to the LBG population.

4. CONCLUSION

We present an analysis of the photometric properties of the $z \sim 3$ LBG spectroscopic sample of Steidel et al. (2003). The relationships between Lyα EW and $(G-\mathcal{R})$ and Lyα EW and $\mathcal{R}$ mag enable a spectral separation of the LBG population using broadband data. We define statistical photometric cuts to reliably generate $\gtrsim 90\%$ pure spectral-type samples of LBGs displaying dominant Lyα in absorption and dominant Lyα in emission. In addition, the spectral-type broadband criteria are extended to isolate clean samples of LAEs.

Our spectroscopic sample of 32 $z \sim 3$ LBGs from the CFHTLS demonstrates the efficiency of the broadband criteria presented here in identifying galaxies based on their Lyα feature, including LAEs. Use of this method will allow the statistical study of $z \sim 3$ galaxies populations from the large numbers easily acquired in deep broadband surveys. This circumvents the expense and constraints of investigations using MOS spectroscopy and the limitations of narrowband searches. Further tests of the criteria, and the extension of the results to other redshifts and filter sets, are presented in a future paper.

J. C. thanks A. E. Shapley for helpful discussions and access to the spectroscopic values. J. C. gratefully acknowledges generous support by Gary McCue.

REFERENCES

Cooke, J., Wolfe, A. M., Gawiser, E., & Prochaska, J. X. 2005, ApJ, 621, 596

Cooke, J., Berrier, J. C., Barton, E. J., Bullock, J. S., & Wolfe, A. M. 2009, MNRAS, submitted

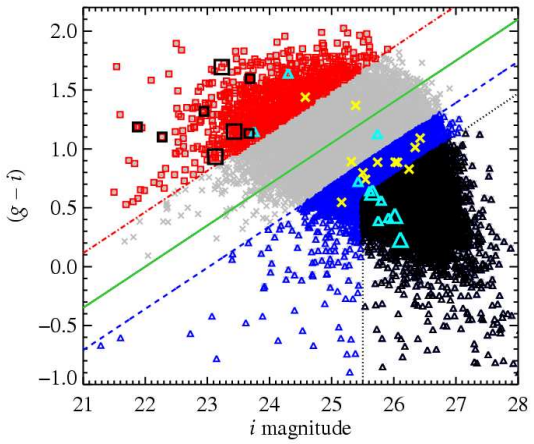

FIG. 4.— $(g-i)$ vs. i-band CMD for u^*gi selected $z \sim 3$ objects in the CFHTLS Deep field "D4" (see the text). Objects are plotted similar to Figure 2 but use light gray (black) triangles to indicate those meeting the adopted LAE criteria. A sample of 32 systems were targeted for spectroscopic follow-up. Black squares mark confirmed aLBGs, black (cyan) triangles mark confirmed eLBGs, and black (yellow) crosses indicate low S/N unidentified systems. Large squares indicate strong absorption and large triangles indicate strong emission. The images are complete to $i \sim 27$ and illustrate the large numbers of each population accessible by this method.

Cooke, J., Sullivan, M., Barton, E. J., Bullock, J. S., Carlberg, R. G., Gal-Yam, A., & Tollerud, E. 2009, Nature, 460, 237
Cowie, L. L., & Hu, E. M. 1998, AJ, 115, 1319
Dawson, S., et al. 2004, ApJ, 617, 707
Fukugita, M., Ichikawa, T., Gunn, J. E., Doi, M., Shimasaku, K., & Schneider, D. P. 1996, AJ, 111, 1748
Gawiser, E., et al. 2006, ApJ, 642, L13
Gawiser, E., et al. 2007, ApJ, 671, 278
Hu, E. M., Cowie, L. L., & McMahon, R. G. 1998, ApJ, 502, L99
Kovač, K., Somerville, R. S., Rhoads, J. E., Malhotra, S., & Wang, J. 2007, ApJ, 668, 15
Lai, K., et al. 2008, ApJ, 674, 70
Le Fèvre, O., et al. 2005, A&A, 439, 845
McCarthy, J. K., et al. 1998, SPIE, 3355, 81
Oke, J. B., Cohen, J. G., Carr, M., Cromer, J., Dingizian, A., Harris, F. H., Labrecque, S., Lucinio, R., Schaal, W., Epps, H., & Miller, J. 1995, PASP, 107, 375
Ouchi, M., et al. 2003, ApJ, 582, 60
Ouchi, M., et al. 2005, ApJ, 620, L1
Reddy, N. A., & Steidel, C. C. 2009, ApJ, 692, 778
Shapley, A. E., Steidel, C. C., Adelberger, K. L., & Pettini, M. 2003, ApJ, 588, 65
Shimasaku, K., et al. 2004, ApJ, 605, L93
Steidel, C. C., Giavalisco, M., Pettini, M., Dickinson, M., & Adelberger, K. L. 1996, ApJ, 462, 17
Steidel, C. C., Adelberger, K. L., Shapley, A. E., Pettini, M., Dickinson, M., & Giavalisco, M. 2003, ApJ, 592, 728
Venemans, B. P., et al. 2005, A&A, 431, 793